

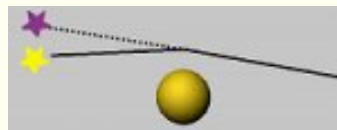
Probing Dark Matter Substructure with Pulsar Timing

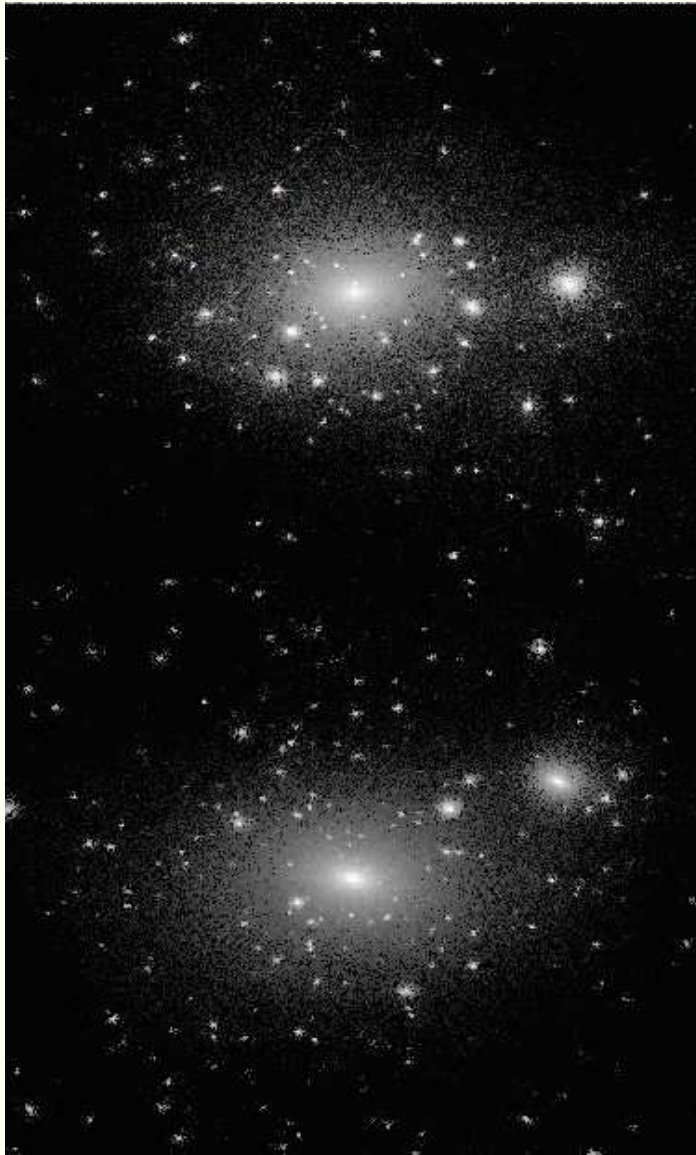
astro-ph/0702546

Ethan Siegel^{1,2}, Mark Hertzberg³, JNF²

¹University of Wisconsin, ²University of Florida, ³MIT

Cosmic Cartography
4 December 2007





$$M = 5 \times 10^{14} M_{\odot}$$

$$R = 2000 \text{ kpc}$$

$$M = 2 \times 10^{12} M_{\odot}$$

$$R = 300 \text{ kpc}$$

Probing Dark Matter Substructure with Pulsar Timing

- Weak Field General Relativity — lensing $\Delta\theta$, Shapiro time delay Δt
- Pulsars
- Pulsar Timing
- Dark Matter Halos
- Dark Matter Halos and Pulsar Timing

Weak Field Gravity

Weak field metric

$$ds^2 = -(1 + 2\phi) dt^2 + (1 - 2\gamma\phi) dx^2$$

Weak Field Gravity

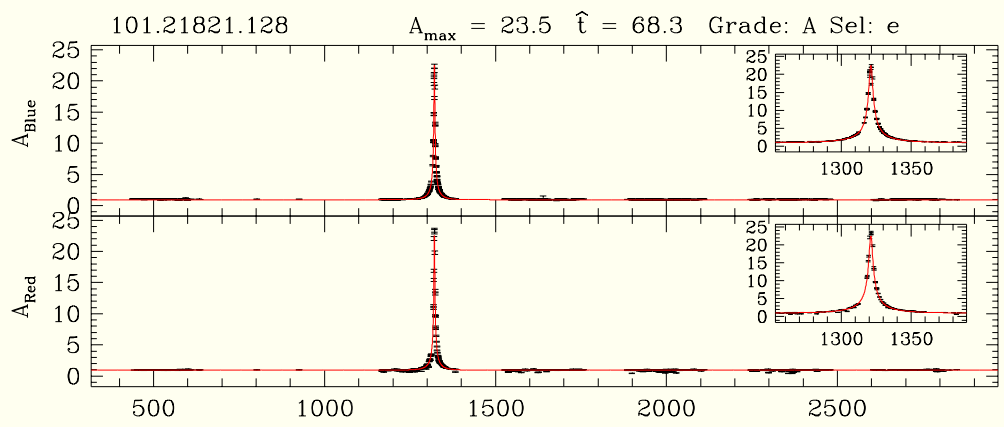
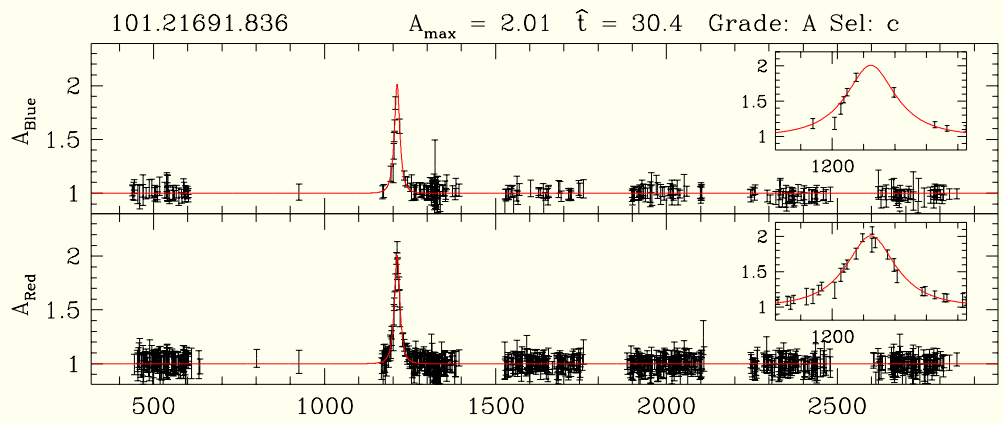
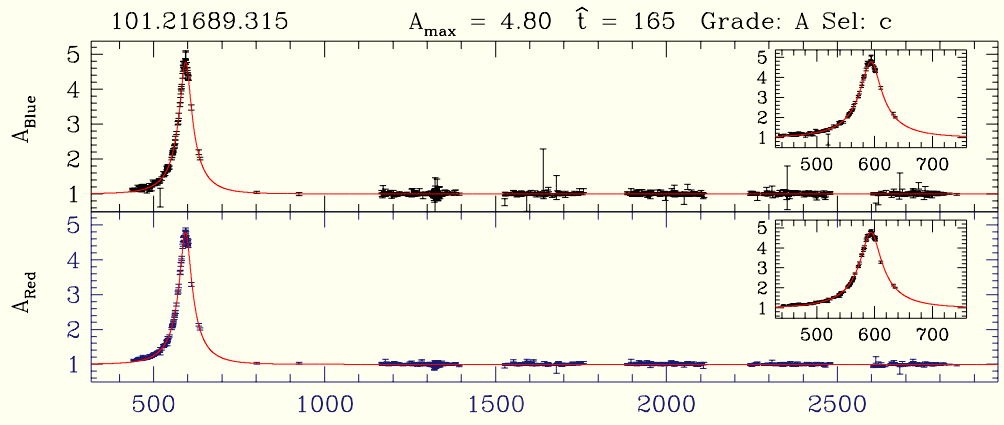
Weak field metric

$$ds^2 = -(1 + 2\phi) dt^2 + (1 - 2\gamma\phi) dx^2$$

Bending of light

$$\Delta\theta = \frac{2(1 + \gamma)GM}{bc^2}$$

F. W. Dyson, A. Eddington, & C. R. Davidson 1920, *Mem. R. A. S.*, 220, 291,
*A Determination of the Deflection of Light by the Sun's Gravitational Field, from
Observations Made at the Total Eclipse of May 29, 1919*



JD - 2448623.5

The MACHO Project

<http://www.macho.mcmaster.ca/>

Weak Field Gravity

Weak field metric

$$ds^2 = -(1 + 2\phi) dt^2 + (1 - 2\gamma\phi) dx^2$$

Bending of light

$$\Delta\theta = \frac{2(1 + \gamma)GM}{bc^2}$$

F. W. Dyson, A. Eddington, & C. R. Davidson 1920, *Mem. R. A. S.*, 220, 291,
*A Determination of the Deflection of Light by the Sun's Gravitational Field, from
Observations Made at the Total Eclipse of May 29, 1919*

Weak Field Gravity

Weak field metric

$$ds^2 = -(1 + 2\phi) dt^2 + (1 - 2\gamma\phi) dx^2$$

Bending of light

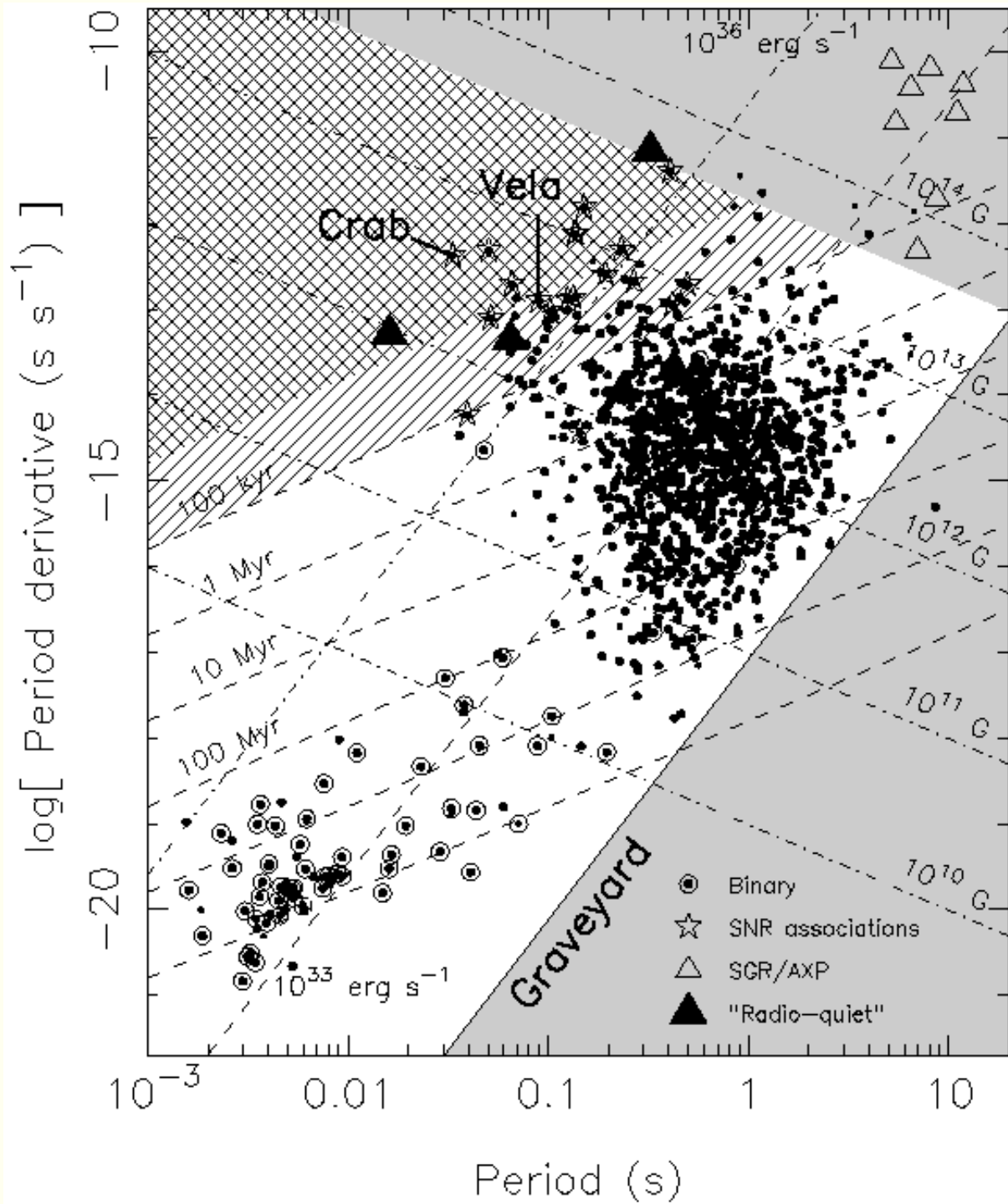
$$\Delta\theta = \frac{2(1 + \gamma)GM}{bc^2}$$

F. W. Dyson, A. Eddington, & C. R. Davidson 1920, *Mem. R. A. S.*, 220, 291,
*A Determination of the Deflection of Light by the Sun's Gravitational Field, from
Observations Made at the Total Eclipse of May 29, 1919*

Shapiro time delay

$$\Delta t = -\frac{(1 + \gamma)GM}{c^3} \ln(1 - \hat{r} \cdot \hat{x})$$

Irwin I. Shapiro, *Phys. Rev. Lett.* 13, 789 (December 1964),
Fourth Test of General Relativity



Taken from "Handbook of Pulsar Astronomy" by Lorimer & Kramer

Pulsar Timing

Steven L. Detweiler 1979, ApJ, 234, 1100, *Pulsar timing measurements and the search for gravitational waves*

Pulse arrival time measurements of pulsars may be used to search for gravitational waves with periods on the order of 1 to 10 years and dimensionless amplitudes of approximately 10^{-11} . The analysis of published data on pulsar regularity sets an upper limit to the energy density of a stochastic background of gravitational waves, with periods of approximately 1 year, which is comparable to the closure density of the universe.

“The arrival time of a pulse a year hence may sometimes be predicted with an uncertainty of only $200 \mu\text{s}$.”

Pulsar Timing

Steven L. Detweiler 1979, ApJ, 234, 1100, *Pulsar timing measurements and the search for gravitational waves*

Pulse arrival time measurements of pulsars may be used to search for gravitational waves with periods on the order of 1 to 10 years and dimensionless amplitudes of approximately 10^{-11} . The analysis of published data on pulsar regularity sets an upper limit to the energy density of a stochastic background of gravitational waves, with periods of approximately 1 year, which is comparable to the closure density of the universe.

“The arrival time of a pulse a year hence may sometimes be predicted with an uncertainty of only $200 \mu\text{s}$.”

Today, this is 200 ns : *TEMPO2, a new pulsar-timing package*

G. B. Hobbs, R. T. Edwards, R. N. Manchester 2006, MNRAS, 369, 655

R. T. Edwards, G. B. Hobbs, R. N. Manchester 2006, MNRAS, 372, 1549

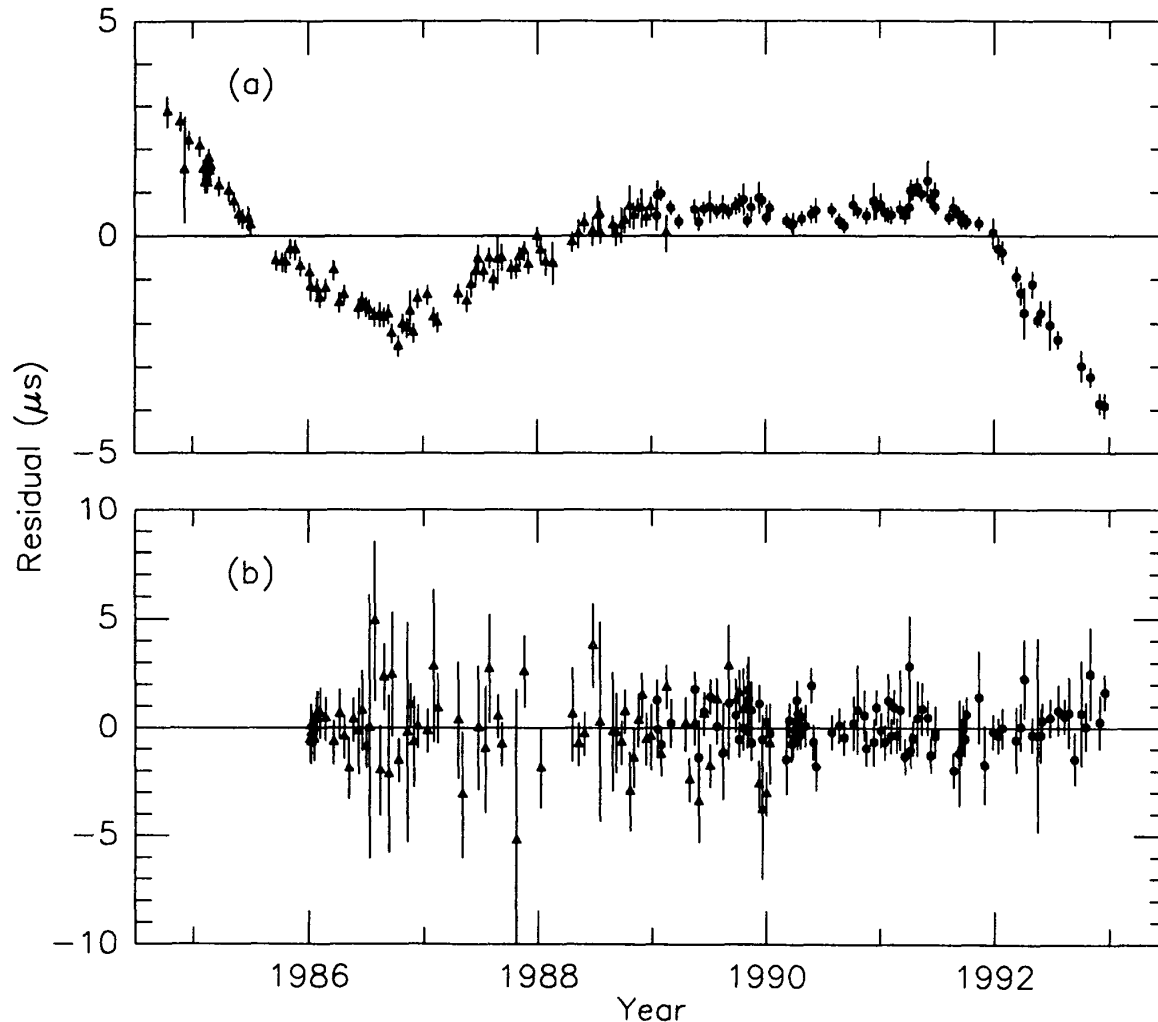


FIG. 5.—Timing residuals for (a) PSR B1937+21 and (b) PSR B1855+09, relative to the parameters listed in Table 2 (with $\dot{\nu} = \dot{\omega} = \dot{x} = \dot{e} = \dot{P}_b = 0$). For clarity we have included only the highest quality data: for PSR B1937+21, the DM-corrected TOAs obtained at 2380 MHz with observing systems B (triangles) and F (filled circles), and for PSR B1855+09, those obtained at 1408 MHz with observing systems A (triangles) and D (filled circles).

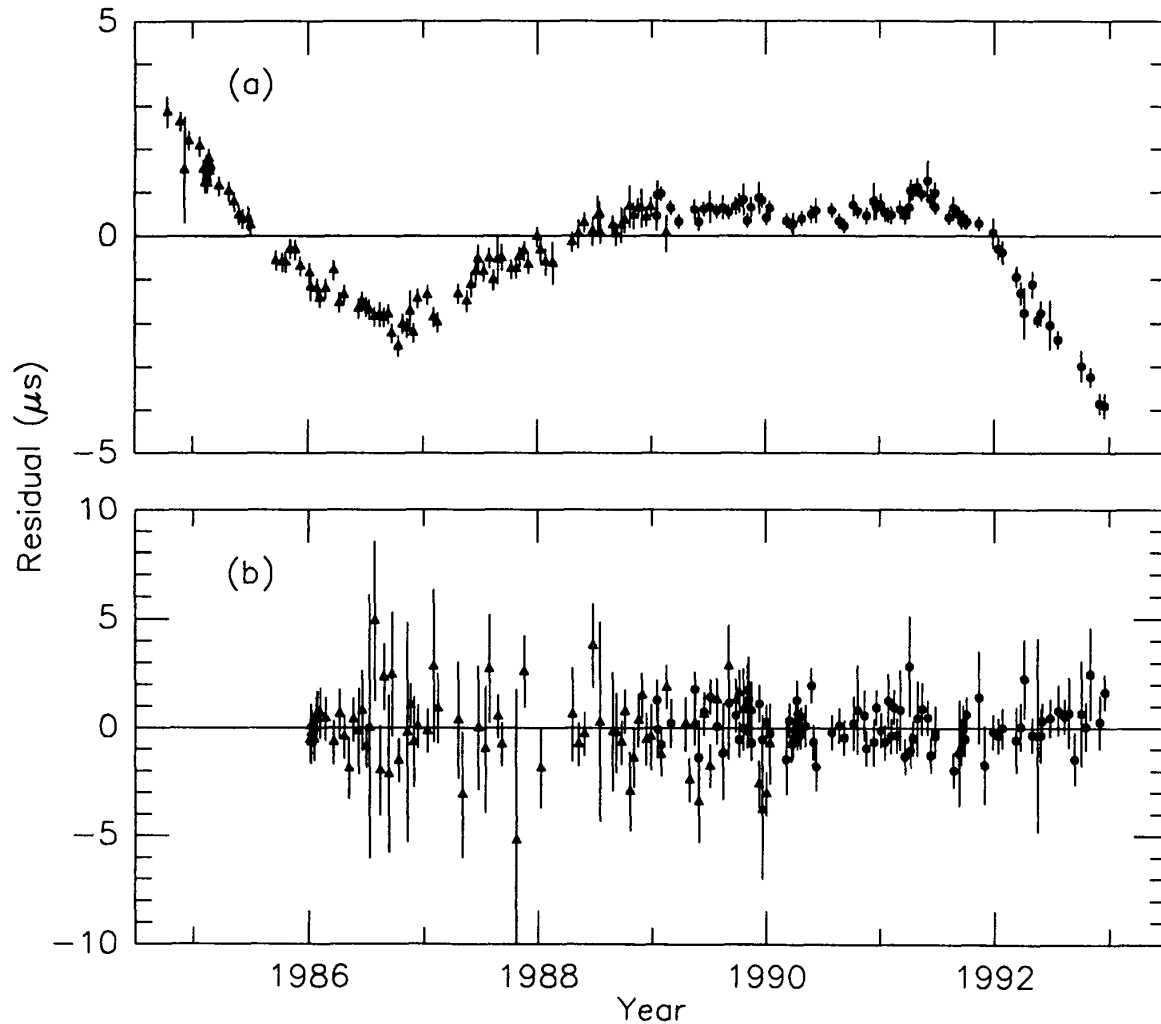


FIG. 5.—Timing residuals for (a) PSR B1937+21 and (b) PSR B1855+09, relative to the parameters listed in Table 2 (with $\dot{\nu} = \dot{\omega} = \dot{x} = \dot{e} = \dot{P}_b = 0$). For clarity we have included only the highest quality data: for PSR B1937+21, the DM-corrected TOAs obtained at 2380 MHz with observing systems B (triangles) and F (filled circles), and for PSR B1855+09, those obtained at 1408 MHz with observing systems A (triangles) and D (filled circles).

$$\dot{G}/G = (-9 \pm 18) \times 10^{-12} \text{ year}^{-1}$$

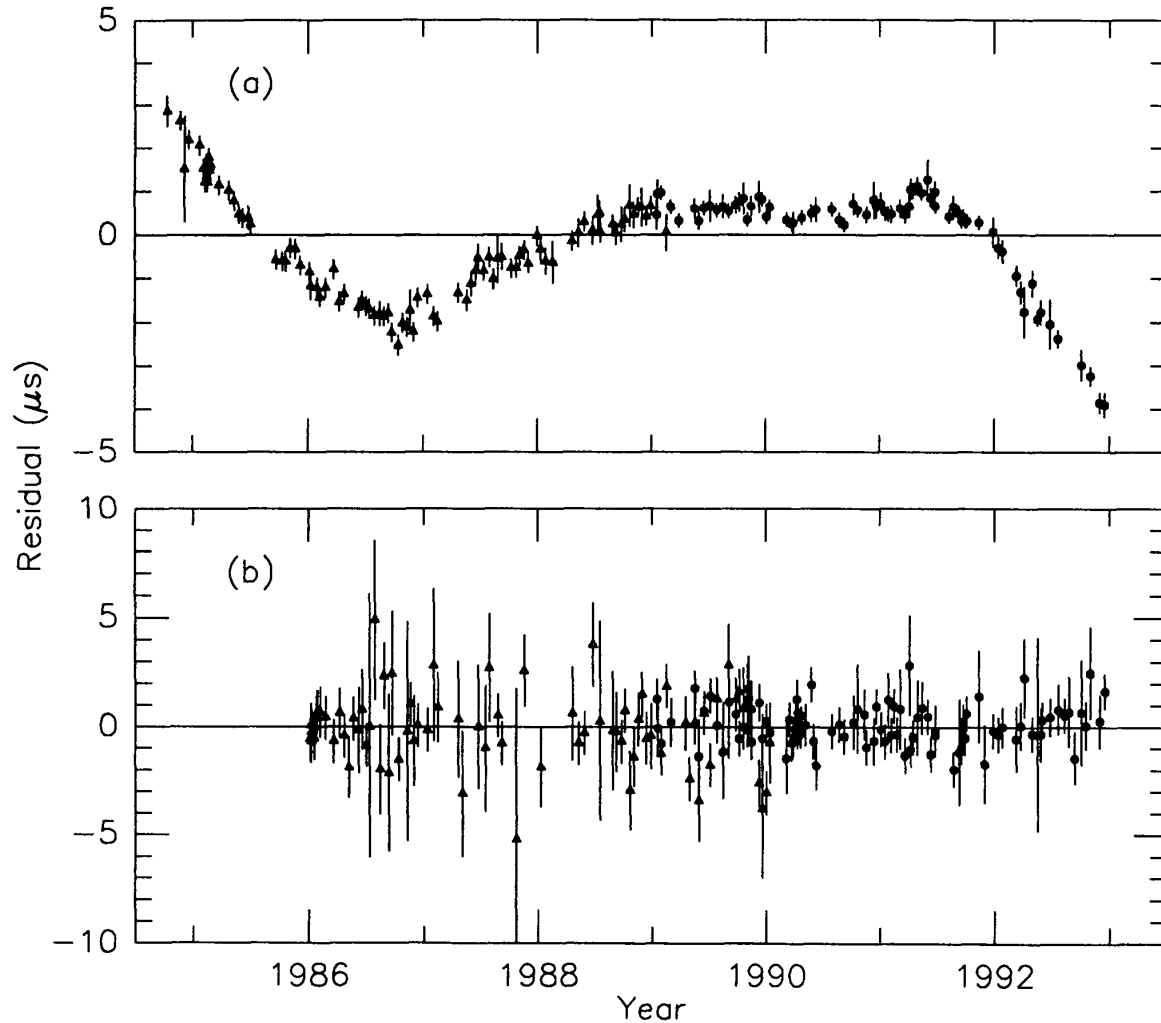


FIG. 5.—Timing residuals for (a) PSR B1937+21 and (b) PSR B1855+09, relative to the parameters listed in Table 2 (with $\ddot{\nu} = \dot{\omega} = \dot{x} = \dot{e} = \dot{P}_b = 0$). For clarity we have included only the highest quality data: for PSR B1937+21, the DM-corrected TOAs obtained at 2380 MHz with observing systems B (triangles) and F (filled circles), and for PSR B1855+09, those obtained at 1408 MHz with observing systems A (triangles) and D (filled circles).

$$\Omega_g h^2 < 6 \times 10^{-8} \text{ (95\% CL)}$$

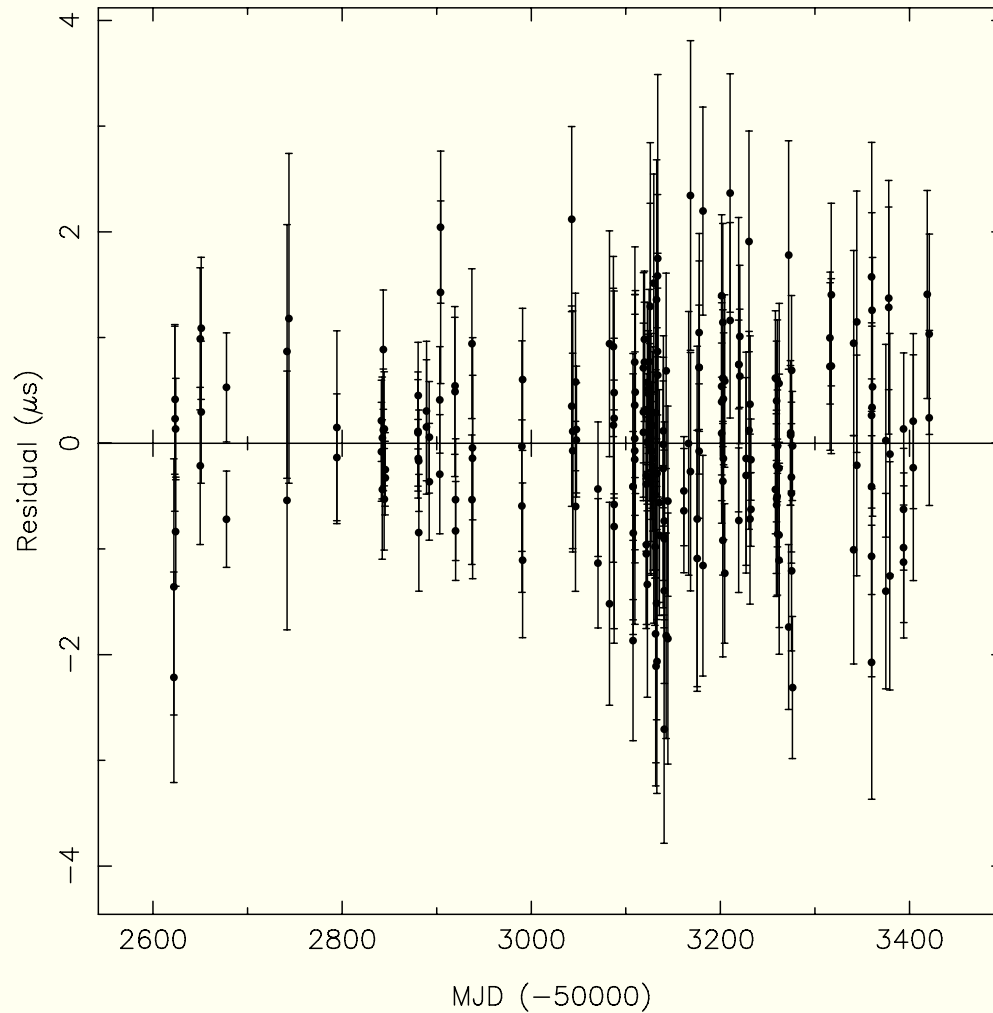


Figure 1. Post-fitting timing residuals for the millisecond pulsar J1600–3053. The spin period of this pulsar is 3.6 ms, the plot displays an obtained rms residual of ~ 650 ns over a period of more than 2 yr. This has been achieved despite the low flux density of the pulsar.

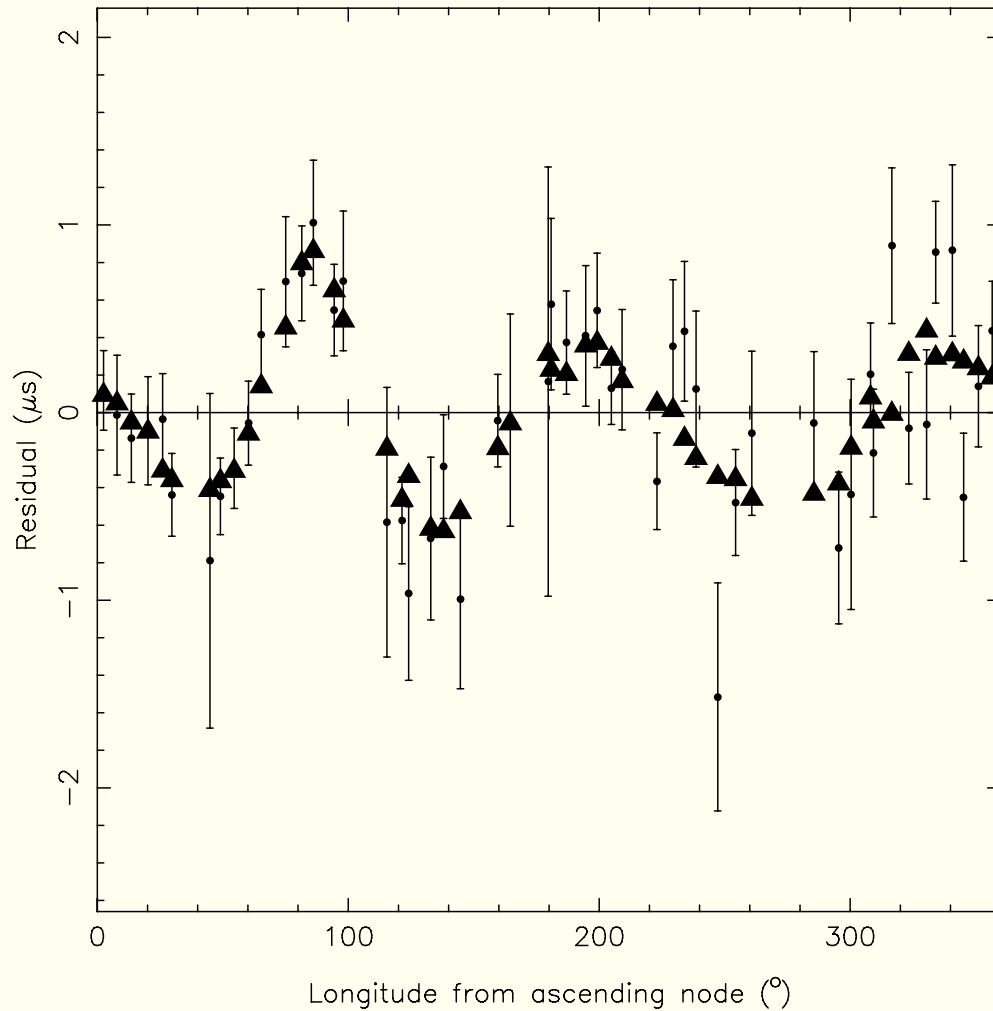
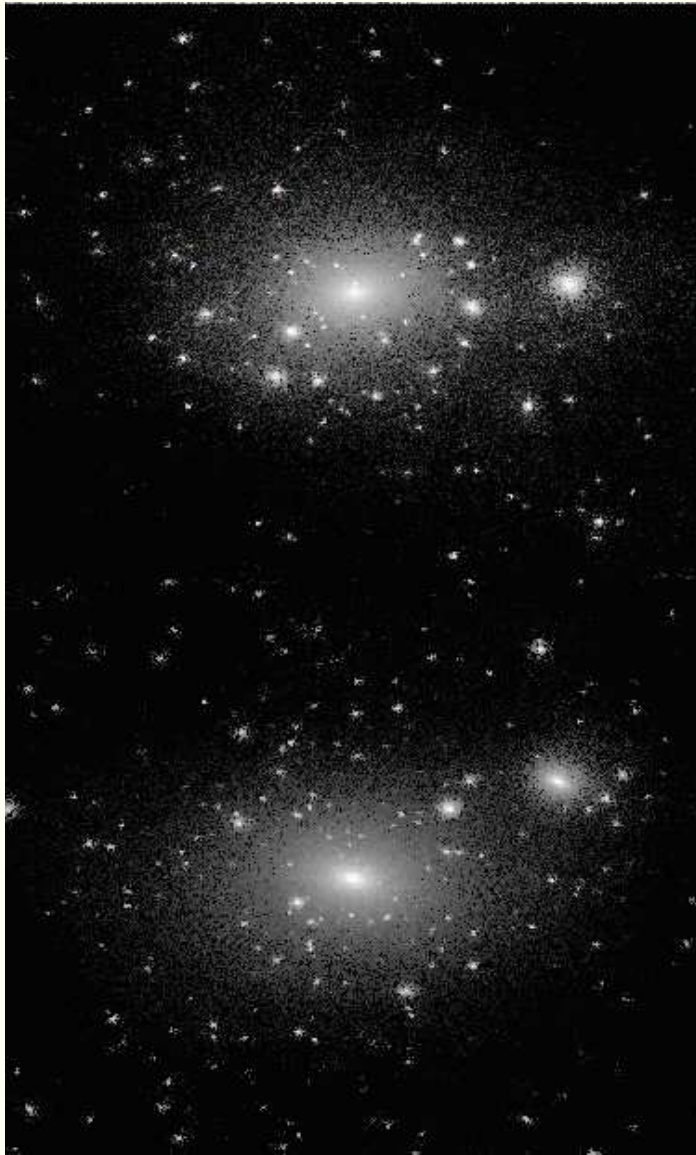


Figure 2. Post-fitting timing residuals for the millisecond pulsar J1600–3053 rebinned into 64 phase bins as a function of longitude, measured from ascending node. Due to uneven phase coverage, the number of data points in each bin is variable. The median number of data points in a bin is 4, the maximum is 12, and 13 bins have no data points. The triangles represent the signature an unmodelled $0.25 M_{\odot}$ companion, and a system inclination of $\sin i = 0.91$ would leave in the data.



$$M = 5 \times 10^{14} M_{\odot}$$

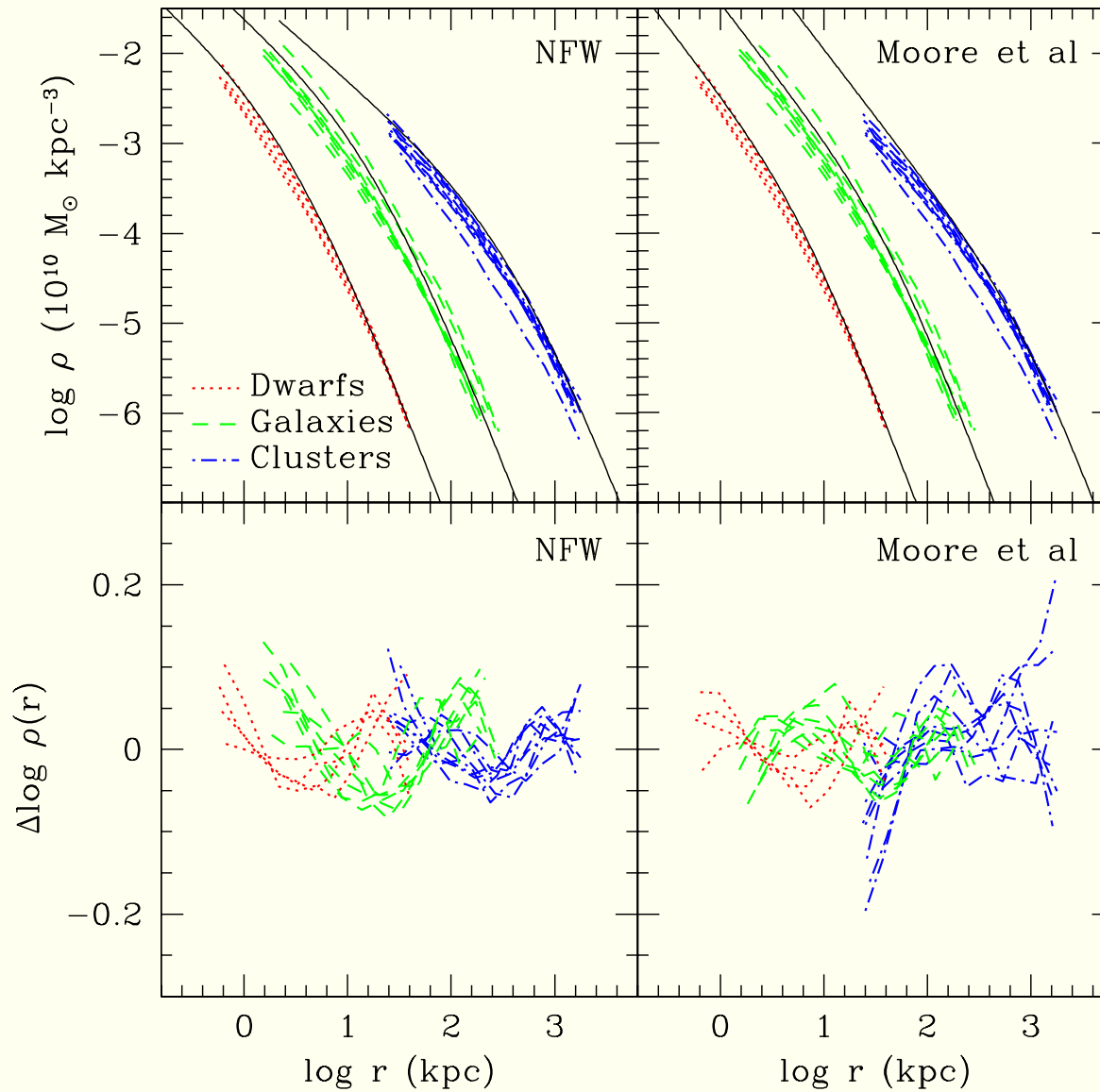
$$R = 2000 \text{ kpc}$$

$$M = 2 \times 10^{12} M_{\odot}$$

$$R = 300 \text{ kpc}$$

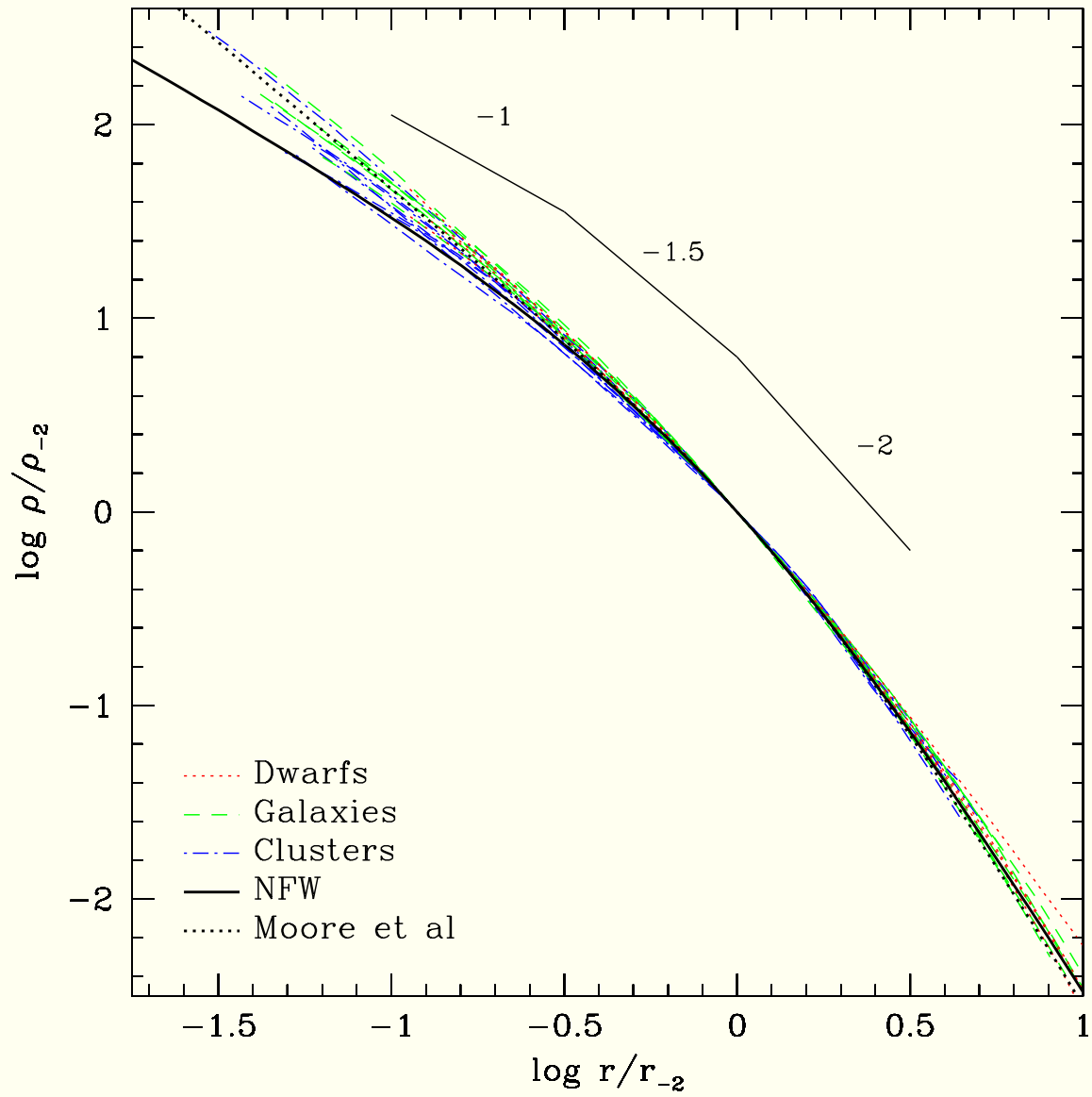
B. Moore et al. 1999, ApJ, 524, 19

Dark Matter Substructure in Galactic Halos

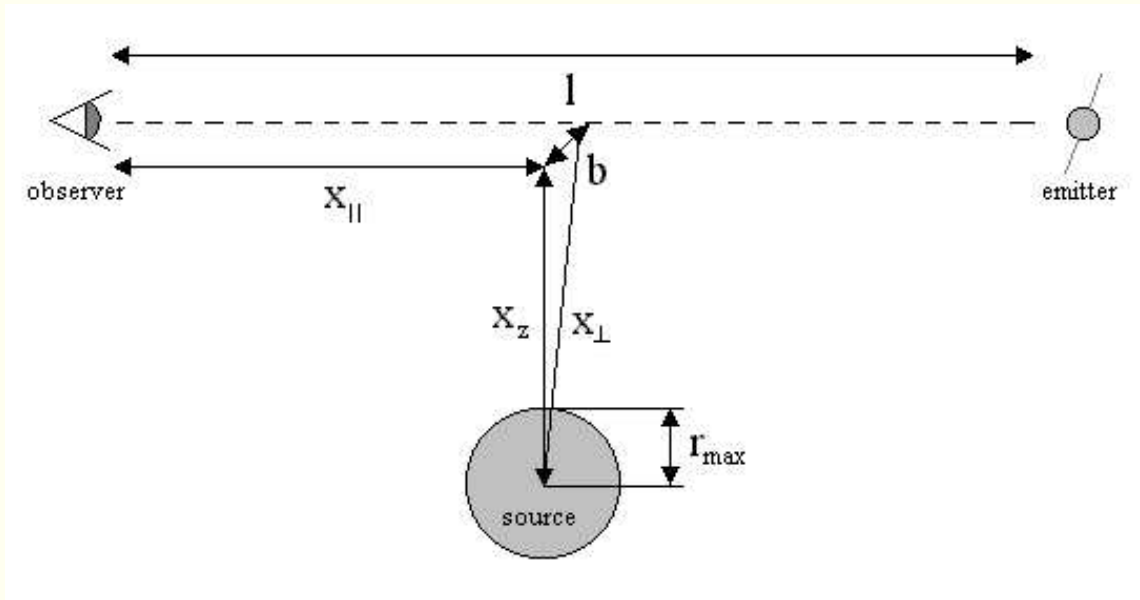


Navarro et al. 2004, MNRAS, 349, 1039.

The inner structure of Λ CDM haloes — III. Universality and asymptotic slopes

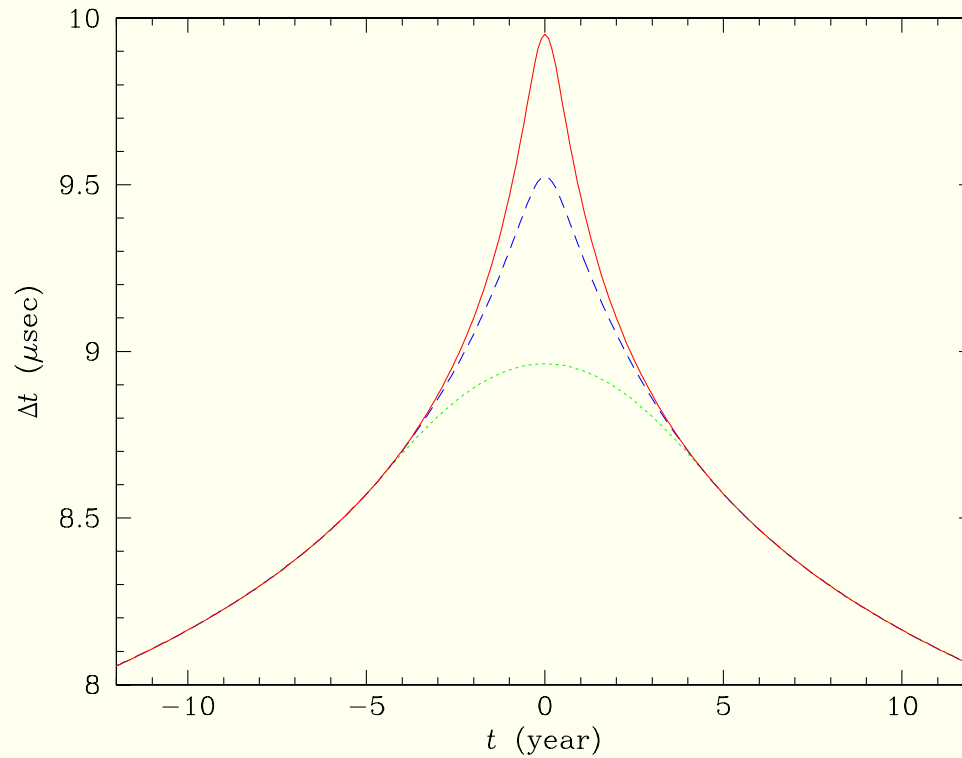


Scaled profiles ρ/ρ_{-2} as a function of r/r_{-2}

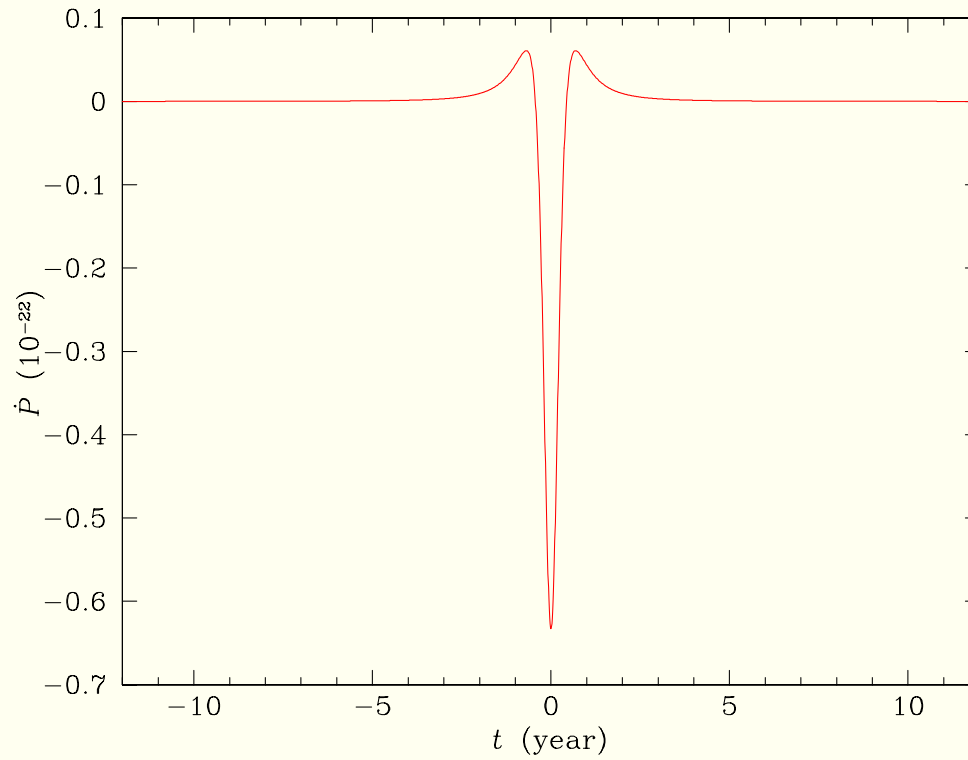


The generic configuration for a fixed emitter and observer, with a gravitational source of radius r_{\max} transiting across or close to the line-of-sight. The emitter-observer distance is l , while the source has a distance to the observer \vec{x} and a velocity \vec{v} , both of which have components perpendicular (x_{\perp} , v_{\perp}) and parallel (x_{\parallel} , v_{\parallel}) to the line-of-sight. The minimum distance between the source and the line-of-sight as the source transits defines the impact parameter, b .

$$\Delta t = \frac{2GM}{c^3} \ln \left[\frac{4x_{\parallel}(l - x_{\parallel})}{x_{\perp}^2} \right] \approx (3 \times 10^{-11} \text{ s}) \left(\frac{M}{M_{\oplus}} \right) \ln \left[\frac{4x_{\parallel}(l - x_{\parallel})}{x_{\perp}^2} \right]$$



Accumulated time delay Δt vs. time for $l = 2 \text{ kpc}$, $x_{\parallel} = 1 \text{ kpc}$, $M = 10^4 M_{\oplus}$, $b = 10^{-4} \text{ pc}$, $v_{\perp} = 200 \text{ km s}^{-1}$, and $T_p = 10^{-3} \text{ s}$. The dashed curved is for a point mass, the solid curve is for a microhalo of constant density with size $r_{\text{max}} = 10^{-3} \text{ pc}$, and the dotted curve is for an extended microhalo with an NFW profile of size $r_{\text{max}} = 10^{-3} \text{ pc}$ and turnover radius $r_0 = 10^{-4.5} \text{ pc}$.

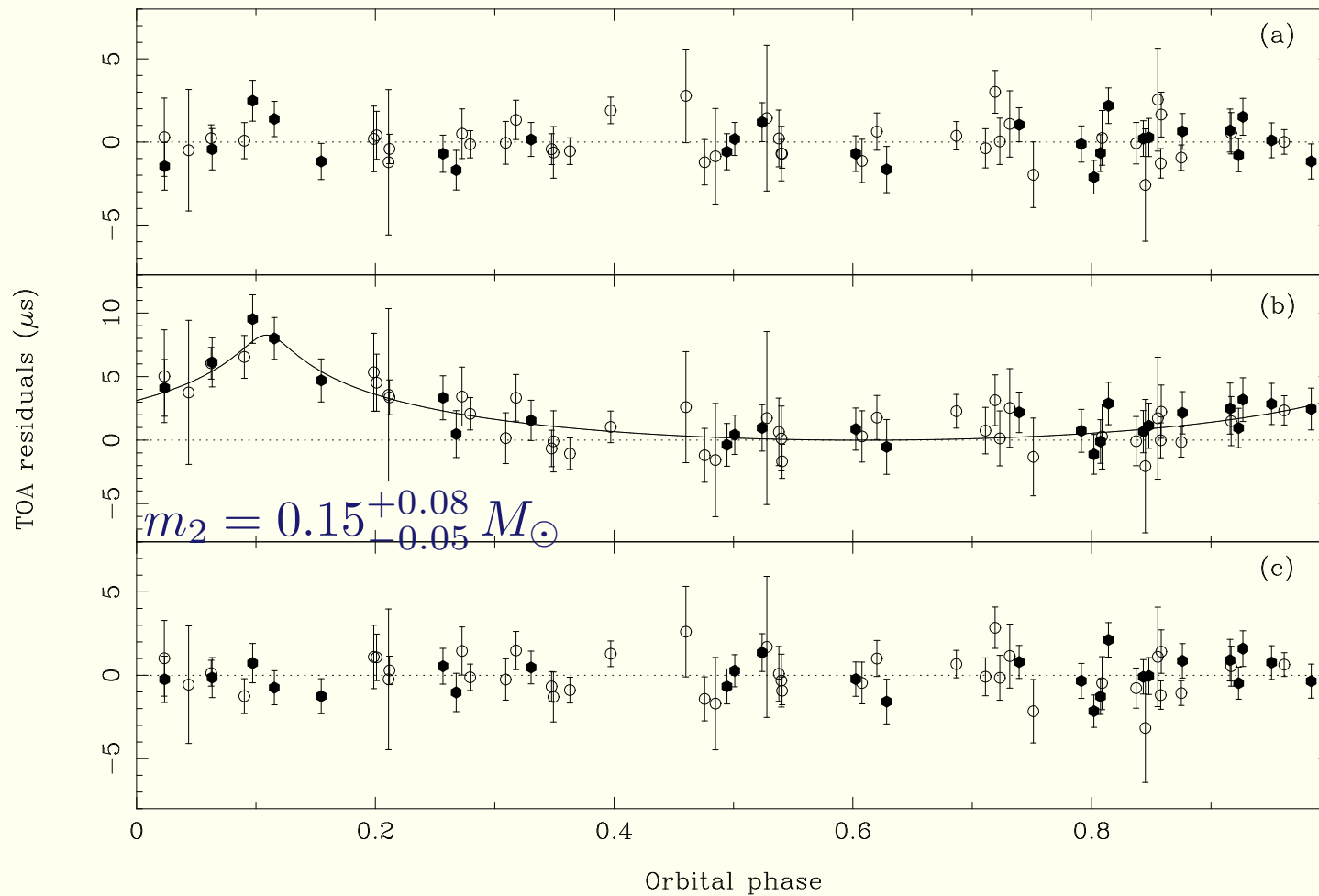


Instantaneous period derivative \dot{P} vs. time for $l = 2$ kpc, $x_{\parallel} = 1$ kpc, $M = 10^4 M_{\oplus}$, $b = 10^{-4}$ pc, $v_{\perp} = 200$ km s $^{-1}$, and $T_p = 10$ μ s (point mass only).

Event Rate

$$\Gamma = n_{\mu\text{H}} \sigma v_{\perp} = 0.011 \left(\frac{n_{\mu\text{H}}}{133 \text{ pc}^{-3}} \right) \left(\frac{b_{\text{max}}}{10^{-4} \text{ pc}} \right) \\ \times \left(\frac{l}{2 \text{ kpc}} \right) \left(\frac{v_{\perp}}{200 \text{ km s}^{-1}} \right) \frac{\text{transits}}{\text{year}}$$

$$n_{\mu\text{H}} = \frac{\rho_{\mu\text{H}}}{10^{-4} M_{\odot}} = 133 \text{ pc}^{-3}$$



Löhmer, Lewandowski, Wolszczan, & Wiełebinski 2006, ApJ, 621, 388.

Shapiro Delay in the PSR J1640+2224 Binary System

The Parkes Pulsar Timing Array Project

R. N. Manchester

arXiv:0710.5026

Detection and study of gravitational waves from astrophysical sources is a major goal of current astrophysics. Ground-based laser-interferometer systems such as LIGO and VIRGO are sensitive to gravitational waves with frequencies of order 100 Hz, whereas space-based systems such as LISA are sensitive in the millihertz regime. Precise timing observations of a sample of millisecond pulsars widely distributed on the sky have the potential to detect gravitational waves at nanohertz frequencies. Potential sources of such waves include binary super-massive black holes in the cores of galaxies, relic radiation from the inflationary era and oscillations of cosmic strings. The Parkes Pulsar Timing Array (PPTA) is an implementation of such a system in which 20 millisecond pulsars have been observed using the Parkes radio telescope at three frequencies at intervals of two – three weeks for more than two years. Analysis of these data has been used to limit the gravitational wave background in our Galaxy and to constrain some models for its generation. The data have also been used to investigate fluctuations in the interstellar and Solar-wind electron density and have the potential to investigate the stability of terrestrial time standards and the accuracy of solar-system ephemerides.

PPTA pulsars and their RMS timing residuals

PSRJ	Pulse Period (ms)	DM (cm^{-3} pc)	Distance (kpc)	Orbital Period (d)	RMS Residual (μs)
J0437–4715	5.757	2.65	0.16	5.74	0.12
J0613–0200	3.062	38.78	0.48	1.20	0.83
J0711–6830	5.491	18.41	1.04	—	1.56
J1022+1001	16.453	10.25	0.40	7.81	1.11
J1024–0719	5.162	6.49	0.53	—	1.20
J1045–4509	7.474	58.15	3.24	4.08	1.44
J1600–3053	3.598	52.19	2.67	14.34	0.35
J1603–7202	14.842	38.05	1.64	6.31	1.34
J1643–1224	4.622	62.41	4.86	147.02	2.10
J1713+0747	4.570	15.99	1.12	67.83	0.19
J1730–2304	8.123	9.61	0.52	—	1.82
J1732–5049	5.313	56.84	1.81	5.26	2.40
J1744–1134	4.075	3.14	0.48	—	0.65
J1824–2452	3.054	119.86	4.90	—	0.88
J1857+0943	5.362	13.31	0.91	12.33	2.09
J1909–3744	2.947	10.39	1.14	1.53	0.22
J1939+2134	1.558	71.04	8.33	—	0.17
J2124–3358	4.931	4.62	0.25	—	2.00
J2129–5721	3.726	31.85	2.55	6.63	0.91
J2145–0750	16.052	9.00	0.50	6.84	1.44

Pulsars may shed light on mysterious dark matter

David Shiga, *New Scientist*, 26 February 2007

<http://space.newscientist.com/article/dn11263-pulsars-may-shed-light-on-mysterious-dark-matter.html>

Pulsar expert Joseph Taylor of Princeton University in New Jersey, US, says detecting dark matter clumps this way would be difficult. “Pulsar timing at that level is not easy,” he told *New Scientist*. “I don’t think it’s likely to produce a convincing detection.” Still, he says it is “conceivable” that such observations, even without a detection, could be used to set a limit on how clumpy dark matter is in our galaxy.

Frederick Jenet of the University of Texas in Brownsville, US, who studies the way passing gravitational waves would distort pulsar signals, agrees. “We can do science with it — we can place limits on the rate of these events happening,” he told *New Scientist*.

Says Jeremiah Ostriker of Princeton: “Any method that has even a remote chance of helping us to determine the nature of the dark matter can be of enormous importance.”